Template-Directed Self-Assembly of 10-*μ*m-Sized Hexagonal Plates

Thomas D. Clark, Rosaria Ferrigno, Joe Tien, Kateri E. Paul, and
George M. Whitesides*

*Contribution from the Department of Chemistry and Chemical Biology, Harvard University,
12 Oxford Street, Cambridge, Massachusetts 02138*

Received January 10, 2002

Abstract: This article presents a strategy for the fabrication of ordered microstructures using concepts of design inspired by molecular self-assembly and template-directed synthesis. The self-assembling components are 4-*μ*m-thick hexagonal metal plates having sides 10 *μ*m in length ("hexagons"), and each template consists of a 4-*μ*m-thick circular metal plate surrounding a central cavity, the perimeter of which is complementary in shape to the external edges of a two-dimensional, close-packed array of hexagons. The hexagons and templates (collectively, "pieces") were fabricated via standard procedures and patterned into hydrophobic and hydrophilic regions using self-assembled monolayers (SAMs). Templated self-assembly occurs in water through capillary interactions between thin films of a nonpolar liquid adhesive coating the hydrophobic faces of the pieces. The hexagons tile the cavities enclosed by the templates, and the boundaries of the cavities determine the sizes and shapes of the assemblies. Curing the adhesive with ultraviolet light furnishes mechanically stable arrays having well-defined morphologies. By allowing control over the structures of the resulting aggregates, this work represents a step toward the development of practical methods for microfabrication based on self-assembly.

Introduction

In this paper we describe the template-directed self-assembly of 10-*μ*m-sized hexagonal metal plates ("hexagons") into ordered arrays having predetermined sizes and shapes. These studies build upon our previous work in mesoscale self-assembly (MESA): self-assembly using forces that operate over distances similar to the dimensions of the components being assembled.[1] MESA based on capillary interactions can form crystalline arrays of nonspherical components with largest dimensions of 10−30 *μ*m;[2] we are developing this general strategy in the belief that it may prove useful in the fabrication of functional devices such as photonic band gap materials[3−6] and self-assembling microelectronic systems.[7−10] The realization of these goals will, however, require control over several attributes of the resulting

assemblies, including the final dimensions and morphologies of the aggregates, the number of component pieces that comprise them, and the spatial arrangement of these pieces with respect to one another. Here, we address these challenges by using appropriately designed templates to direct the self-assembly process.

Template is a general term for a scaffold or guide that is used to arrange objects with the aim of influencing the outcome of a subsequent process. For example, a chemical template is a species that organizes an assembly of atoms with respect to one or more geometric loci in order to achieve a particular linking of atoms.[11] The replication of DNA is an example of chemical templating by a molecular species,[12] and emulsion-templated synthesis of porous solids is an instance of templating by a supramolecular assembly.[13] Oriented single crystals template the deposition of thin crystalline layers in molecular beam epitaxy,[14] and colloidal crystals can function as sacrificial templates in the synthesis of inverse opaline materials.[15]

In recent years, several groups have applied the concepts of chemical templating to the self-assembly of components much larger than individual atoms or molecules. Wiltzius and van

* To whom correspondence should be addressed. E-mail: gwhitesides@gmwgroup.harvard.edu.

(1) Bowden, N. B.; Weck, M.; Choi, I. S.; Whitesides, G. M. *Acc. Chem. Res.* **2001**, *34*, 231−238.
(2) Clark, T. D.; Tien, J.; Duffy, D. C.; Paul, K. E.; Whitesides, G. M. *J. Am. Chem. Soc.* **2001**, *123*, 7677−7682.
(3) A useful introduction for the layperson to the field of photonic crystals: Yablonovitch, E. *Sci. Am.* **2001**, *December*, 46−55.
(4) Joannopoulos, J. D.; Meade, R. D.; Winn, J. N. *Photonic Crystals: Molding the Flow of Light*; Princeton University Press: Princeton, NJ, 1995.
(5) Blanco, A.; Chomski, E.; Grabtchak, S.; Ibisate, M.; John, S.; Leonardo, S. W.; Lopez, C.; Meseguer, F.; Miguez, H.; Mondia, J. P.; Ozin, G. A.; Toader, O.; Van Driel, H. M. *Nature* **2000**, *405*, 437−440.
(6) Vlasov, Y. A.; Bo, X. Z.; Sturm, J. C.; Norris, D. J. *Nature* **2001**, *414*, 289−293.
(7) Terfort, A.; Whitesides, G. M. *Adv. Mater.* **1998**, *10*, 470−473.
(8) Gracias, D. H.; Tien, J.; Breen, T. L.; Hsu, C.; Whitesides, G. M. *Science* **2000**, *289*, 1170−1172.
(9) Boncheva, M.; Gracias, D.; Jacobs, H.; Whitesides, G. M. *Proc. Natl. Acad. Sci. U.S.A.* **2002**, in press.

(10) Jacobs, H. O.; Tao, A. R.; Schwartz, A.; Gracias, D. H.; Whitesides, G. M. *Science* **2002**, *296*, 323−325.
(11) Anderson, S.; Anderson, H. L.; Sanders, J. K. M. *Acc. Chem. Res.* **1993**, *26*, 469−475.
(12) Watson, J. D.; Crick, F. H. C. *Nature* **1953**, *171*, 964−967.
(13) Imhof, A.; Pine, D. J. *Nature* **1997**, *389*, 948−951.
(14) Herman, M. A.; Sitter, H. *Molecular beam epitaxy: fundamentals and current status*, 2nd ed.; Springer-Verlag: New York, 1996.
(15) Xia, Y. N.; Gates, B.; Yin, Y. D.; Lu, Y. *Adv. Mater.* **2000**, *12*, 693−713.

Blaaderen employed lithographically fabricated reliefs to direct the formation of bulk colloidal crystals with predetermined sizes and lattice structures,[16] and Pouliqen et al. extended this strategy to the crystallization of 2-mm-sized spheres.[17] Xia used holes in flat substrates, designed to accommodate a discrete number of spherical colloids, to generate aggregates with defined sizes and structures.[18,19] Smith demonstrated shape-selective integration of microelectronic device elements into textured substrates via fluidic self-assembly (FSA).[20,21] Velev has exploited the spatial confinement afforded by liquid droplets to direct the crystallization of colloidal spheres,[22−24] and we have used a related method—templated MESA based on capillary interactions at the interface between two liquids—to generate spherical[25] and quasi-two-dimensional structures.[26,27] Similar approaches by Xia, Ozin, and others have included the crystallization of spherical colloids through confinement in microchannels,[15,28,29] and the selective placement of small objects on patterned surfaces using chemical,[30,31] magnetic,[32] electrostatic,[33] and capillary[34] interactions.

Previously, we used capillarity to generate untemplated arrays from 10-μm-sized metallic plates.[2] We patterned the surfaces of the plates into hydrophobic and hydrophilic regions using self-assembled monolayers (SAMs) and coated the hydrophobic regions with thin films of a nonpolar liquid adhesive; in water, capillary forces between the adhesive films provided the attractive forces necessary for assembly. Although the resulting aggregates were internally well ordered, our inability to control their external morphologies represented a potential limitation to this method (Figure 1a). Here, we explore an approach to overcoming this limitation that employs templates to control the sizes and shapes of the structures formed by the self-assembly of 10-μm-sized hexagons (Figure 1b).

Experimental Design

Each template consists of a 4-μm-thick circular metal plate enclosing a central cavity intended to accommodate a discrete
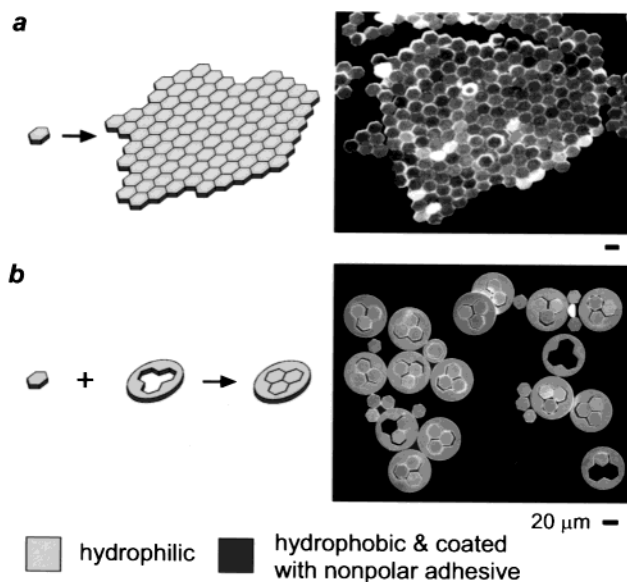

Figure 1. Comparison of untemplated and templated self-assembly of 4-μm-thick hexagonal metal plates having sides 10-μm-long; the scale bar is the same for the two images. In both cases, the components self-assemble in water through capillary interactions between thin layers of a nonpolar liquid adhesive precipitated selectively onto their hydrophobic surfaces.[2] (a) In the absence of a template, the hexagons self-assemble into arrays that are internally well-ordered but irregular in size and shape. (b) In templated self-assembly, the hexagons tile the cavity enclosed by a circular template. The edges of the cavity present "binding sites" for the attachment of hexagons, and the boundaries of the cavity define the sizes and shapes of the resulting assemblies.

number of 4-μm-thick hexagons (Figure 1b). Conceptually, we designed each template by subtracting the shape formed by a 2-D, close-packed array of hexagons from the center of a solid circle; templated self-assembly constitutes the reverse process: tiling of the resulting cavity with an array of hexagons. The edges of the cavities ("binding sites") act as nucleation points during self-assembly and stabilize the growing arrays against mechanical damage by anchoring them to the templates. We designed the binding sites to be slightly larger than the hexagons in order to accommodate the adhesive layer at the interface between the pieces. From our previous work, we estimated the thickness of the adhesive to be on the order of 100 nm;[2] thus, for hexagons with sides 10 μm in length, we expected an optimal fit to result if the corresponding linear dimensions of the binding sites were 10.2 μm, or 2% larger than those of the hexagons (vide infra).

We fabricated the hexagons and templates (collectively, "pieces") using photolithography and electrodeposition as previously reported (Figure 2a).[2] Starting with a silicon wafer coated sequentially with a thin film of Cr, Ag, Cr, and Au, photolithography generated molds for the electrodeposition of Au. Evaporation of Cr onto the electrodeposited Au, dissolution of the Ag sacrificial layer to release the pieces, and sonication to debur them yielded hexagons and templates comprised of a 4-μm-thick layer of Au with a thin film of Cr coating their top and bottom faces. The Cr surfaces formed a hydrophilic native oxide (Cr/Cr$_2$O$_3$),[35] and we rendered the exposed Au surfaces hydrophobic by treatment with an ethanolic solution of hexadecanethiol (HDT) to generate alkanethiolate SAMs.[36]

(16) van Blaaderen, A.; Ruel, R.; Wiltzius, P. *Nature* **1997**, *385*, 321−324.
(17) Pouliquen, O.; Nicolas, M.; Weidman, P. D. *Phys. Rev. Lett.* **1997**, *79*, 3640−3643.
(18) Yin, Y.; Xia, Y. *Adv. Mater.* **2001**, *13*, 267−271.
(19) Yin, Y. D.; Lu, Y.; Gates, B.; Xia, Y. N. *J. Am. Chem. Soc.* **2001**, *123*, 8718−8729.
(20) Yeh, H.-J. J.; Smith, J. S. *IEEE Photonics Technol. Lett.* **1994**, *6*, 706−708.
(21) (a) Stix, G. *Sci. Am.* **2001**, *March*, 20. (b) http://www.alientechnology.com.
(22) Velev, O. D.; Furusawa, K.; Nagayama, K. *Langmuir* **1996**, *12*, 2374−2384.
(23) Velev, O. D.; Furusawa, K.; Nagayama, K. *Langmuir* **1996**, *12*, 2385−2391.
(24) Velev, O. D.; Lenhoff, A. M.; Kaler, E. W. *Science* **2000**, *287*, 2240−2243.
(25) Huck, W. T. S.; Tien, J.; Whitesides, G. M. *J. Am. Chem. Soc.* **1998**, *120*, 8267−8268.
(26) Choi, I. S.; Bowden, N.; Whitesides, G. M. *J. Am. Chem. Soc.* **1999**, *121*, 1754−1755.
(27) Choi, I. S.; Weck, M.; Xu, B.; Jeon, N. L.; Whitesides, G. M. *Langmuir* **2000**, *16*, 2997−2999.
(28) Yang, S. M.; Ozin, G. A. *Chem. Commun.* **2000**, 2507−2508.
(29) Ozin, G. A.; Yang, S. M. *Adv. Funct. Mater.* **2001**, *11*, 95−104.
(30) Aizenberg, J.; Braun, P. V.; Wiltzius, P. *Phys. Rev. Lett.* **2000**, *84*, 2997−3000.
(31) Demers, L. M.; Park, S. J.; Taton, T. A.; Li, Z.; Mirkin, C. A. *Angew. Chem., Int. Ed. Engl.* **2001**, *40*, 3071−3073.
(32) Murakami, Y.; Idegami, K.; Nagai, H.; Kikuchi, T.; Morita, Y.; Yamamura, A.; Yokoyama, K.; Tamiya, E. *Mater. Sci. Eng. C* **2000**, *12*, 67−70.
(33) Bohringer, K. F.; Goldberg, K.; Cohn, M.; Howe, R.; Pisano, A. Parallel Microassembly with Electrostatic Force Fields. In *Proceedings of the 1998 IEEE International Conference on Robotics and Automation*; Leuven, Belgium, May 16−20, 1998; IEEE: New York, 1998; 98CH36146, 1204−1211.
(34) Srinivasan, U.; Liepmann, D.; Howe, R. T. *J. Microelectromech. Syst.* **2001**, *10*, 17−24.

(35) Kubaschewski, O.; Hopkins, B. E. *Oxidation of Metals and Alloys*; Buttersworths: London, 1962.
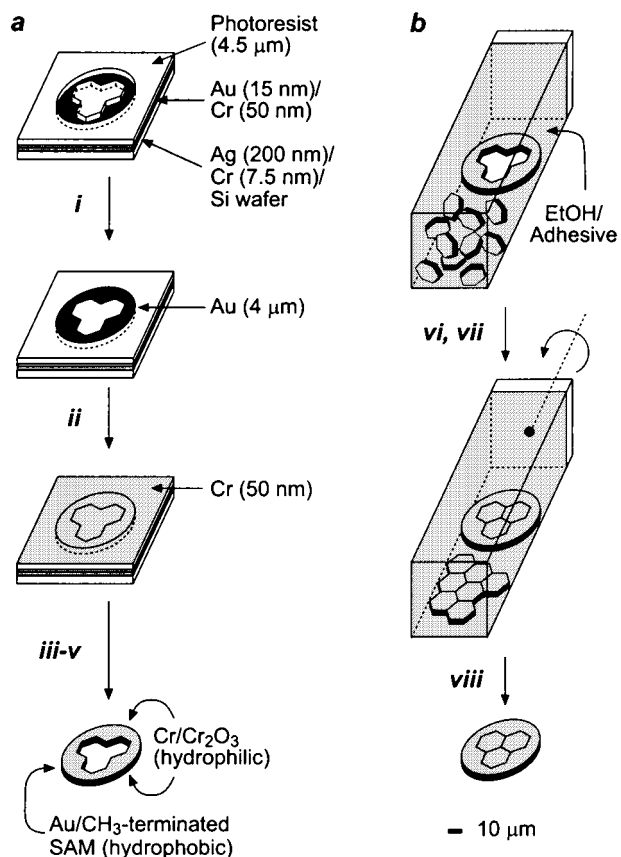(36) Ulman, A. *Chem. Rev.* **1996**, *96*, 1533−1554.

Figure 2. (a) Fabrication of the templates and 10-μm-sized hexagons (collectively, "pieces"). (i) Electrodeposition through patterned photoresist on a Si/SiO$_2$/Cr/Ag/Cr/Au electrode formed 4-μm-thick gold pieces. (ii) We evaporated chromium (50 nm) onto the pieces. (iii) Dissolution of the silver film with nitric acid released the pieces and (iv) sonication in ethanol removed the residual thin films of chromium extending from their edges. (v) Treatment with a 10 mM ethanolic solution of HS(CH$_2$)$_{15}$CH$_3$ formed a hydrophobic SAM on the gold surfaces; the chromium surfaces formed a hydrophilic native oxide layer (Cr/Cr$_2$O$_3$).[35] (b) Templated self-assembly. (vi) We placed ∼10^3 templates and ∼3 × 10^5 hexagons in a 3 mL glass cuvette containing 50 μL of a ∼0.1% ethanolic solution of nonpolar photocurable adhesive. Slow addition of water diluted the ethanol, precipitated the lubricant selectively onto the hydrophobic faces of the pieces, and caused the pieces to aggregate. The adhesive-coated pieces and 3 mL of water remained in the cuvette. (vii) We rotated the cuvette axially at 100−200 rpm for 12−24 h; this rotation provided the annealing force that allowed the initially formed aggregates to coalesce into ordered arrays. (viii) After assembly, exposure to UV radiation (λ ∼ 254 nm) furnished mechanically stable arrays that could be removed for examination.

A typical experiment began by placing ∼10^3 templates and an approximately 100-fold stoichiometric excess of hexagons together in a glass cuvette and treating them with an ethanolic solution of a nonpolar liquid adhesive (Figure 2b; the details of this procedure are described in the Experimental Section). Dilution of the ethanol with water caused the adhesive to precipitate and selectively coat the hydrophobic faces of the pieces; axial rotation of the cuvette provided the agitation that allowed the self-assembly to proceed. When two adhesive-coated faces contacted each other, the liquid films merged, prompting the pieces to align through capillarity in order to minimize the area of the resulting adhesive−water interface. The self-assembly typically reached completion within 12−24 h. After curing the adhesive with ultraviolet light, we confirmed the structures of the aggregates using optical and scanning electron microscopy (SEM). The yields of the assemblies were deter-

mined by dividing the number of full templates by the total number of templates observed; to avoid skewing the results through additional handling, we did not attempt to purify the assemblies.

Results

We focused our initial efforts on optimizing the fit of the hexagons to the templates. According to our fabrication scheme, the sizes of the pieces are determined by the sizes of the molds used for electrodeposition (Figure 2a). We began, therefore, by adjusting the photolithographic conditions used to generate the molds, and then tested the resulting pieces in self-assembly experiments. Because the tolerance of the features on our photomasks was only ±0.5 μm,[37] we were unable to adjust the absolute sizes of the pieces arbitrarily by simply designing new masks. Instead, we adjusted the relative sizes of the pieces by varying other photolithographic conditions, including the tone of photoresist used and the parameters of exposure and development,[38−40] until we obtained hexagons and templates that were appropriately matched in size—that is, the linear dimensions of the templates were a few percent larger than those of the hexagons. A representative example of this refinement process is shown in Figure 3.

Figure 4 presents schematic and SEM images of four templated assemblies prepared using optimized photolithographic conditions as described in the Experimental Section. The simplest template was intended to accommodate a single hexagon and consists of a solid circle surrounding a hexagonal cavity (**1**); we also designed templates for trimeric (**2**), heptameric (**3**), and nonadecameric (**4**) assemblies. In all cases, the pieces self-assembled to give well-ordered arrays in good yields (Figure 4). By contrast, we obtained less ordered aggregates in significantly lower yields when the pieces were mismatched in size.

We explored the self-assembly process by using optical microscopy to examine the "reaction mixtures" at various times during the course of a single experiment. Within a few seconds after precipitating the adhesive onto the pieces, most of the hexagons organized themselves into small, untemplated arrays oriented randomly with respect to each other; these arrays were single-layered and contained ∼10−100 hexagons each. The templates had bound few hexagons by this point and contained many vacancies. As the assembly proceeded, the untemplated arrays coalesced into larger, multilayered assemblies, each containing ∼10^4−10^5 hexagons, and the vacancies in the templates began to fill. These observations suggest the following mechanism for the templated self-assembly. In the early stages of an experiment, the hexagons aggregate quickly to produce arrays that are too large and irregularly shaped to bind stably

(37) The chrome/soda lime glass photomasks employed in this study were fabricated using a laser imager and wet development and etch procedures; the nominal overall resolution of these processes is ±0.5 μm. Advance Reproductions, Inc., North Andover, MA (www.advancerepro.com). Personal communication, 2001.
(38) Over-exposure and/or over-development of a positive photoresist can broaden features relative to the photomask.[39] This broadening increases the size of the hexagons while *decreasing* the size of the binding sites on the templates. (b) Negative photoresists such as SU-8 that rely upon cross-linking reactions tend to yield features that are slightly smaller than those on the photomask due to shrinkage of the photoresist following exposure.[40]
(39) Madou, M. J. *Fundamentals of Microfabrication: The Science of Miniaturization*; 2nd ed.; CRC Press LLC: Boca Raton, FL, 2002.
(40) Lorenz, H.; Despont, M.; Fahrni, N.; Brugger, J.; Vettiger, P.; Renaud, P. *Sens. Actuator A−Phys.* **1998**, *64*, 33−39.
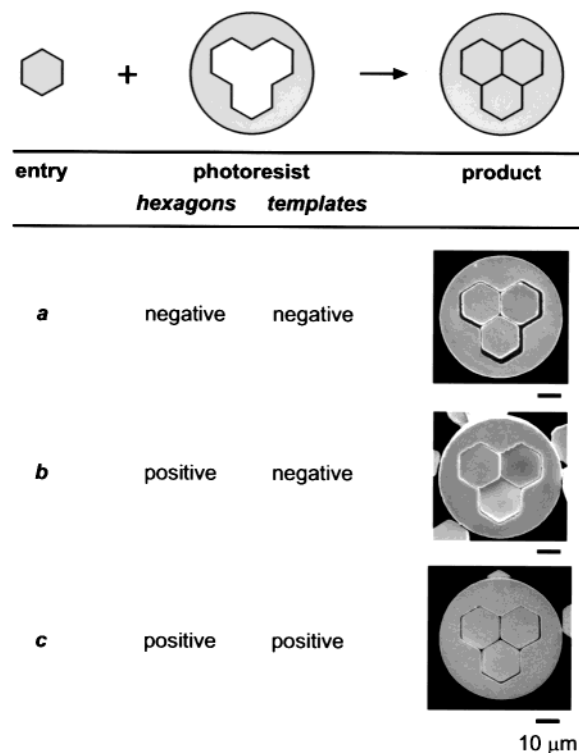
Figure 3. Optimization of the photolithographic conditions used to prepare a respresentative hexagon/template couple. The scale bar is the same for each image. We designed the hexagonal features on the photomasks for the hexagons to have sides 10 μm in length; the corresponding features on the photomasks for the templates were designed to have linear dimensions 5% larger. (a) The use of negative photoresist for both the hexagons and templates gave hexagons that were too small for the binding sites.[38a] (b) When we tried to assemble templates prepared using negative photoresist with hexagons generated using positive photoresist, we found that the hexagons were too large for the binding sites.[38b] (c) We obtained pieces that were appropriately matched in size by carefully controlling the parameters of exposure and development and used a positive photoresist for both the hexagons and templates.[39]

to the templates; this aggregation also rapidly decreases the concentration of free hexagons and small assemblies capable of filling the binding cavities. As they grow in size, the untemplated assemblies experience increasingly forceful collisions with their surroundings. These collisions dislodge single hexagons and small aggregates, which in turn bind to vacant sites on the templates.

The results presented in Figure 4 demonstrate the success of our strategy for producing aggregates of defined sizes and shapes. We note, however, that the assemblies formed by templates **1**–**4** display external morphologies that are reminiscent of untemplated assemblies (Figure 1a).[2] As a demonstration of the versatility of our method, we used templating to generate a structure having an unusual shape that does not form stably in untemplated experiments (Figure 5). Template **5** was designed to produce a linear assembly containing a 60° bend; we reasoned that the higher aspect ratio of this assembly relative to those shown in Figure 4 would render it more vulnerable to fracture in the absence of a template. Significantly, we have not observed the formation of a similar V-shaped aggregate in untemplated experiments.[2] The design of **5** proved successful and allowed the generation of the expected array **5a**, which contains 30 hexagons. This result highlights an important concept of design in these systems: the notion that stabilizing interactions between
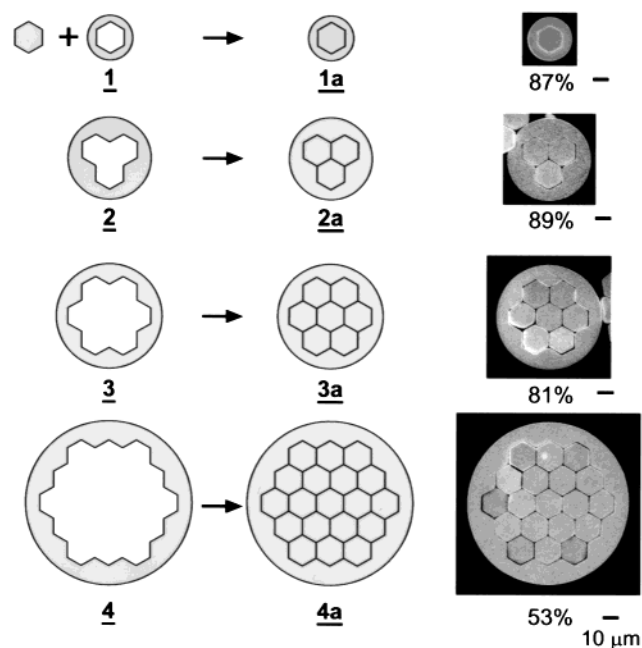

Figure 4. Schematic illustration of four templates and SEM images of the corresponding templated assemblies. We estimated the percent yield of each assembly by counting ∼100 templates and dividing the number of fully formed assemblies by the total number of templates observed. The scale bar is the same for each image.

the external edges of the assemblies and the binding sites on the templates can be used to tailor the shapes of the resulting aggregates.

Discussion

The templated assemblies presented here are single-layered, close-packed arrays of hexagons; we anticipate, however, that our approach will extend to multilayered arrays, and to the self-assembly of components having a variety of shapes.[2] Although we made no attempt to purify the templated assemblies, we expect that the use of techniques such as sizing and differential sedimentation will allow us to isolate the desired products and recycle the untemplated arrays and defective aggregates.

Defects in the templated assemblies consisted of two types: assemblies containing vacancies (Figures 1b and 6a) and assemblies containing extra hexagons (Figure 6b). Vacancies were more common in larger assemblies (e.g., **4a** and **5a**) than in smaller ones; we believe that this trend reflects, in part, the greater susceptibility of larger assemblies to mechanical damage under the agitation conditions used. Many templated assemblies, however, contained only one or a small number of vacant sites; we believe that such vacancies are unlikely to have arisen from mechanical damage, and may have been caused by the low concentration of free hexagons and small aggregates capable of filling the binding cavities. For example, monomeric assembly **1a** is small and, presumably, stable; nevertheless, **1a** displayed a vacancy rate of 13% (Figure 3), most likely due to the low concentration of free hexagons during the self-assembly process.[41]

In an effort to reduce the number of vacancies in the templated assemblies, we examined two methods intended to

(41) We were unable to obtain **1a** in quantitative yield even after extended "reaction" times (∼4 days), possibly due to slow polymerization of the adhesive layer during the course of the experiments.
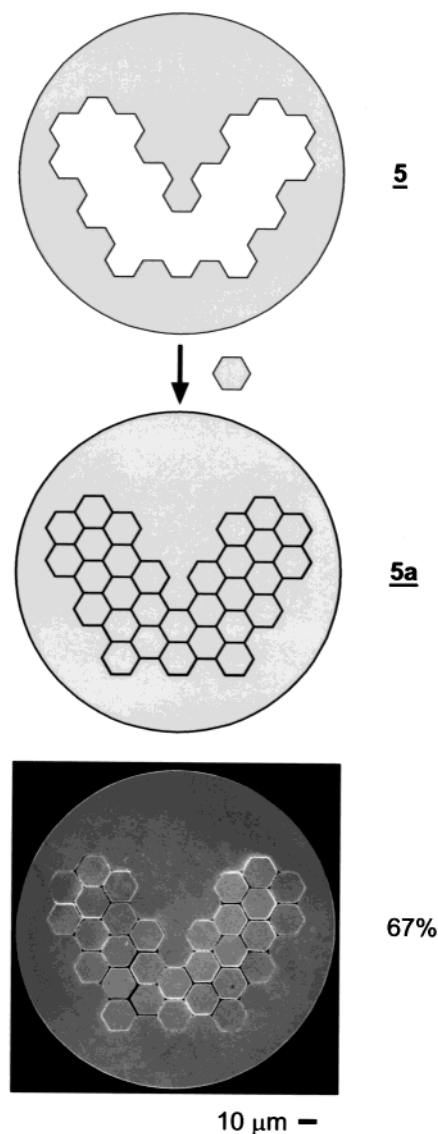
Figure 5. Schematic illustration of the V-shaped template **5** and SEM image of the resulting assembly **5a**, which contains 30 hexagons.

increase the concentration of free hexagons. For the first method, we precipitated the adhesive simultaneously onto the hexagons and templates, allowed the pieces to self-assemble for some time, and then added fresh hexagons; for the second method, we precipitated the adhesive onto the templates only, and then added fresh hexagons and allowed the pieces to assemble. In both cases, the course of the self-assembly was indistinguishable from that observed previously: the hexagons aggregated quickly into untemplated arrays with few unassociated hexagons remaining, and the binding cavities on the templates filled slowly and incompletely. The failure of these methods may have resulted from the persistence of excess adhesive in the reaction vessels, perhaps in the form of microscopic droplets adventitiously attached to the walls of the cuvette, which then coated the hexagons and allowed them to assemble. The complete elimination of vacancies will likely require pieces that self-assemble only in the presence of a template; we are currently examining ways of designing such pieces.

The second type of defect—arrays containing one or more extra hexagons attached at unintended locations—likely arises from small differences in thickness among the pieces. In our
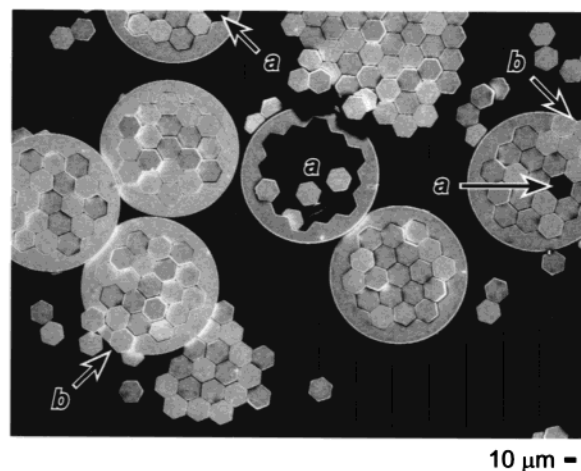

Figure 6. Examples of the two major classes of defects observed in the templated assemblies, as shown here for nonadecameric assembly **4a** (Figure 4). (a) Templates containing vacancies. (b) Templates containing one or more extra hexagons attached at unintended sites.

earlier study, we found that electrodeposited Au typically varies in thickness by ±10% over the surface of a wafer;[2] here, this variation produces hexagons and templates having hydrophobic faces that differ in height from piece to piece. When the pieces assemble, portions of their adhesive-coated faces remain exposed to water, presenting partial binding sites to which extra hexagons may adhere weakly.[42] We minimized these defects by employing vigorous agitation to remove the extra hexagons. Under these conditions, this type of defect occurred in only ∼5% of the templated assemblies; for the purpose of calculating yields, we considered these assemblies full. Complete elimination of these defects would require either that the pieces be uniformly thick or that the thickness of the hydrophilic layers on the top and bottom of each piece be greater than or equal to the variation in thickness among the pieces. For example, we expect that pieces bearing a ≥0.8-μm-thick layer of Cr on their top and bottom faces would produce arrays free from this type of defect.

The results presented in Figures 4 and 5 suggest that the structures of the templates can strongly influence the stabilities of the corresponding assemblies. For example, the yields of assemblies **1a**−**4a** (**1a** ≈ **2a** > **3a** > **4a**) correlate inversely with the number of hexagons that comprise them. We believe that this correlation indicates that the small assemblies are more stable than the large ones under the agitation conditions used. The yield of assembly **5a** is, however, greater than that of **4a** (67% vs 53%), even though the former contains more hexagons (30 vs 19). We rationalize this observation by considering not only the number of hexagons in the assemblies but also the number of binding sites on the templates. In this context, we define a "binding site" as an edge in the binding cavity of a template to which one edge of a hexagon binds. For example, template **1** (Figure 4) contains 6 binding sites, which together bind a single hexagon. Figure 7 shows a plot of the ratio (number of binding sites on the templates/number of hexagons in the resulting assemblies) vs the yields of the assemblies. The observed positive correlation suggests that the stability of the assemblies increases with increasing number of binding sites per hexagon. We note that, because the yields shown in Figures

(42) We believe that variation in thickness among pieces is also at least partly responsible for the formation of multilayered, untemplated aggregates observed in these experiments, as well as in our previous study.[2]
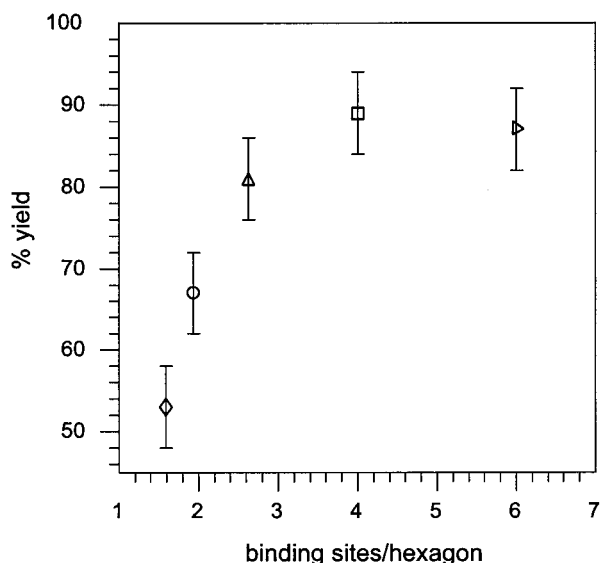
Figure 7. Plot of the ratio (no. of binding sites on a template/no. of hexagons in the corresponding assembly) vs the yields of the templated assemblies: **4a** (◇), **5a** (○), **3a** (△), **2a** (□), and **1a** (rotated triangle) (Figures 4 and 5; see text for the definition of "binding site"). The error bars were constructed by using a conservative estimate of the error in the percentage yields of these assemblies (a fixed error of ±5% yield). The observed positive correlation suggests that increasing the number of binding sites per hexagon increases the stability of the templated assemblies. This correlation must be considered tentative, however, because the yields determined for these assemblies represent results from single experiments.

4 and 5 represent results from single experiments, this correlation must be regarded as tentative.

Conclusion

Using principles of design inspired by template-directed chemical synthesis, we have developed a strategy for the fabrication of ordered microstructures having well-defined sizes and shapes. Our approach separates the fabrication into two distinct steps: preparation of the components and their self-assembly into larger structures. Although the pieces described here are composed of gold and chromium, we anticipate that this method will extend to components prepared from a variety of materials; one potential application lies in the integration of micro-device elements made from incompatible substances. In this context, we note that a related process—fluidic self-assembly (FSA)—is currently being developed for the incorporation of optoelectronic elements into flexible polymeric substrates.[20,21]

This work represents a step toward the realization of practical methods for microfabrication based on self-assembly. Because capillary interactions become stronger at smaller size scales relative to other forces,[43] we anticipate that these techniques will also prove useful in preparing structures at the nanoscale. Our ultimate goal is to develop efficient methods for the fabrication of small, functional devices. In other work, we have already used capillarity to form electrical contacts in the millimeter[7−9] and 280-μm-size regimes,[10] and Howe and co-workers reported a similar strategy for the attachment of micromachined silicon parts to patterned substrates.[34] We are currently working to extend the strategy described here to the fabrication of micro- and nanostructured devices such as microelectromechanical systems (MEMS)[44−50] and photonic band gap crystals.[3−6]

Experimental Section

Chemicals. All chemicals and solvents were used as supplied from the indicated vendors. Cr and Ag evaporation sources were purchased from Alfa Aesar, and Au evaporation sources from Materials Research Corp. We obtained 453 developer and SJR5440 and SU-8-5 photoresists from Microchem Corp. (Newton, MA). Propylene glycol methyl ether acetate (PGMEA), benzoin isobutyl ether, 1,6-hexanediol diacrylate, mercaptohexadecanoic acid (MHA), and hexadecanethiol (HDT) were acquired from Aldrich. Dodecyl methacrylate was purchased from Polysciences, Inc. (Warrington, PA). Gold electroplating solutions (Techni-25E) were obtained from Technic, Inc. (Cranston, RI). We purchased concentrated nitric acid and acetone from VWR Scientific, and absolute EtOH from Pharmco (Brookfield, CT).

Fabrication of the Substrates. Substrates for photolithography consisted of silicon wafers (2 in., ⟨100⟩, test grade, 13−17 mils, 1−10 Ω cm; Silicon Sense, Nashua, NH) coated sequentially with 7.5 nm of Cr, 200 nm of Ag, 50 nm of Cr, and 20 nm of Au using an electron beam evaporator.[39]

Spin-Coating. Substrates for use with the positive photoresist SJR-5440 were primed by immersion for 5 min in a 2 mM ethanolic solution of 85:15 mol % HDT/MHA to promote adhesion of the photoresist. We rinsed the substrates with ethanol, sonicated them for 1 min in clean-room-grade acetone, and rinsed them with acetone followed by 18 MΩ water. Residual water was removed under a stream of nitrogen, and the wafers were dried by placing them for 30 s on a digital hotplate set at 105 °C. We spin-coated[39] the wafers with SJR5440 photoresist at 500 rpm for 5 s, accelerated them to 3200 rpm at 2000 rpm s^{-2}, and spun them an additional 30 s to give a 4.5-μm-thick film. The wafers were placed directly onto a digital hotplate set at 105 °C, baked for 1 min, then promptly removed and held under ambient conditions for ≥30 min before exposure.

We primed the substrates for use with the negative photoresist SU-8-5 by immersion for 5 min in a 2 mM ethanolic solution of 90:10 mol % MHA/HDT to promote adhesion of the photoresist; substrates were cleaned and dried as above. We spin-coated[39] the wafers with SU-8-5 at 500 rpm for 5 s, accelerated them to 3500 rpm at 2000 rpm s^{-2}, and spun them an additional 15 s to give a 5-μm-thick film. The wafers were baked for 1 min on a digital hotplate set at 65 °C, then transferred promptly to another hotplate set at 90 °C. After 3 min at 90 °C, we turned off the heating element and allowed the wafers to reach room temperature slowly over ∼15 min.

Fabrication of the Photomasks. The photomasks were fabricated from chromium and soda lime glass by Advance Reproductions, Inc. (North Andover, MA).[37] Masks for use with positive and negative photoresists were fabricated in dark and clear field, respectively,[39] and patterns for the hexagons and each of the templates were produced on separate masks. We generated the patterns for the photomasks using a CAD program (AutoSketch 6.0, Autodesk, Inc.). As provided to the mask manufacturer, the features consisted of regular hexagons having sides 10.0 μm in length and templates having corresponding linear dimensions 5% larger; for example, we designed the cavity of template **1** to be a regular hexagon having sides 10.5-μm-long.

(43) Fearing, R. S. Survey of Sticking Effects for Micro Parts Handling. In *Proceedings of the 1995 IEEE/RSJ International Conference on Intelligent Robots and Systems. Human Robot Interaction and Cooperative Robots*; Pittsburgh, PA, August 5−9, 1995; IEEE Comput. Soc. Press: Los Alamitos, CA, 1995; 95CB35836, pp 212−217.

(44) Syms, R. R. A.; Yeatman, E. M. *Electron. Lett.* **1993**, *29*, 662−664.
(45) Green, P. W.; Syms, R. R. A.; Yeatman, E. M. *J. Microelectromech. Syst.* **1995**, *4*, 170−176.
(46) Syms, R. R. A. *Sens. Actuator A−Phys.* **1998**, *65*, 238−243.
(47) Syms, R. R. A.; Gormley, C.; Blackstone, S. *Sens. Actuator A−Phys.* **2001**, *88*, 273−283.
(48) Harsh, K. F.; Bright, V. M.; Lee, Y. C. *Sens. Actuator A−Phys.* **1999**, *77*, 237−244.
(49) Dahlmann, G. W.; Yeatman, E. M. *Electron. Lett.* **2000**, *36*, 1707−1708.
(50) Lubecke, V. M.; Barber, B.; Chan, E.; Lopez, D.; Gross, M. E.; Gammel, P. *IEEE Trans. Microw. Theory Technol.* **2001**, *49*, 2093−2098.

Photolithography. Photolithography[39] was performed in a class-100 clean room in the absence of ambient ultraviolet light using a Suss MJB 3 mask aligner in contact mode, with a 350 W mercury lamp set at 10 mW cm^{-2} ($\lambda = 405$ nm).

(a) Photolithography for Monomeric Assembly 1a. For template **1**, we exposed a 4.5-μm-thick film of SJR5440 photoresist for 18 s using a dark-field photomask. We then immersed the wafer in fresh 453 developer contained in a 100-mm-diameter glass Petri dish. Using a pair of tweezers, we gently agitated the wafer. Within 3 min, the exposed regions began to exude a red color, indicating that development of the photoresist had begun. The agitation was continued until formation of the red color ceased and the resulting pattern attained a uniform appearance ($\sim$10 min total). After rinsing thoroughly with 18 MΩ water, we dried the wafer under a stream of N$_2$.

For the hexagons, the use of SJR5440 photoresist resulted in hexagons that were too large for the binding sites,[38a] but the use of SU-8-5 gave hexagons that were appropriately matched to the binding sites.[38b] We exposed at 5-μm-thick film of SU-8-5 photoresist for 12 s using a clear-field photomask. We then placed the wafer directly onto a digital hotplate set at 65 °C. After baking 3 min at 65 °C, we quickly transferred the wafer to another digital hotplate set at 95 °C and baked an additional 5 min. The heating element was then turned off, and the wafer was allowed to reach room temperature slowly over $\sim$15 min. We developed the wafer by immersion in fresh PGMEA contained in a 70-mm-diameter glass crystallization dish. The dish was gently swirled by hand until the pattern in the photoresist became uniform ($\sim$45 s); we then rinsed the wafer thoroughly with PGMEA and dried it under a stream of N$_2$.

(b) Photolithography for Trimeric Assembly 2a. We performed the photolithography used to fabricate both the hexagons and templates using SJR5440 photoresist as described above for template **1**.

(c) Photolithography for Heptameric Assembly 3a. We performed the photolithography used to fabricate both the hexagons and templates using SJR5440 photoresist as described above for template **1**.

(d) Photolithography for Nonadecameric Assembly 4a. We performed the photolithography used to fabricate both the hexagons and templates using SJR5440 photoresist as described above for template **1**.

(e) Photolithography for V-Shaped Assembly 5a. For template **5**, we over-exposed a 4.5-μm-thick film of SJR5440 photoresist for 30 s using a dark-field photomask in order to decrease the size of the binding sites relative to the features on the photomask.[38a] The wafer was developed as described above for template **1**.

We performed the photolithography for the hexagons using SU-8-5 photoresist as described above for the hexagons used to generate assembly **1a**.[38b]

Electrodeposition. Prior to electrodeposition, we cleaned the substrates for 5 min in a UV/ozone cleaner to remove the SAM primer and any residual photoresist. We electrodeposited Au from a gold sulfite bath (Techni-25E, 1 Tr oz Au gal^{-1}) at 60 °C with a platinum anode. The solution was stirred at 300 rpm, and the current density was maintained at 1 mA cm^{-2}; under these conditions, a 1-μm-thick film of gold formed in $\sim$16 min. We continued the electrodeposition for a total of 64 min to produce a 4-μm-thick film of Au.

Isolation and Derivatization of the Pieces. After electrodeposition, we rinsed the wafers with deionized water, dried them under a stream of N$_2$, and treated them for 5 min with UV/ozone to clean the surface of the electrodeposited Au. We then evaporated 50 nm of Cr onto the wafers using an electron beam evaporator.[39]

Before etching the Ag sacrificial layers, we removed the SJR5440 photoresist from the wafers by sonication in acetone; we subjected wafers patterned with SU-8-5 directly to the etching conditions. The wafers were etched with 35% aqueous HNO$_3$ at room temperature to remove the pieces.[51] We rinsed away the etchant and sonicated the pieces in EtOH to break apart the residual thin films of Cr. After

sonication, we allowed the pieces to settle, decanted the excess thin flakes of Cr, and sonicated the pieces again; repetition of this procedure 4–5 times yielded pieces that were free of Cr flakes.

Prior to derivatizing the pieces with SAMs, we cleaned their metal surfaces using piranha solution ($\sim$2:1 v/v concentrated H$_2$SO$_4$:30% H$_2$O$_2$)[52] at room temperature for 5 min; we found that prolonged exposure to piranha led to irreproducibility in the formation of alkanethiolate SAMs, likely due to the formation of thick oxide layers (Au$_2$O$_3$) on the Au surfaces.[53-56] *Caution: Piranha solution is extremely corrosive and potentially explosive when in contact with oxidizable materials.*[57,58] When we omitted this cleaning step, the pieces tended to adhere to one another through their (nominally hydrophilic) Cr faces during self-assembly, presumably due to the presence of hydrophobic contaminants on the Cr surfaces (e.g. residual photoresist); cleaning the pieces with piranha solution abolished these undesired interactions. After thoroughly rinsing away the piranha with water, we incubated the pieces in EtOH for 30 min at room temperature to reduce any Au$_2$O$_3$ that had formed on the Au surfaces.[53-56] Subsequent treatment with 10 mM HDT in EtOH for several hours generated hydrophobic alkanethiolate SAMs on the Au faces;[36] formation of the native oxide (Cr$_2$O$_3$)[35] rendered the Cr faces hydrophilic.

Self-Assembly. Using a pasteur pipet, we transferred $\sim$10^3 templates and an approximately 100-fold stoichiometric excess of hexagons to a $1 \times 1 \times 3$ cm glass cuvette. After rinsing the pieces thoroughly with EtOH to remove excess thiol, we filled the cuvette with 3 mL of EtOH, added $\sim$30 μL of a photocurable adhesive (96:2:2 w/w/w dodecyl methacrylate/benzoin isobutyl ether/1,6-hexanediol diacrylate),[7] and stirred the EtOH until the adhesive had fully dissolved. We then allowed the pieces to settle into one corner of the cuvette and, using a pasteur pipet, withdrew nearly all of the ethanol/adhesive solution, leaving only enough to cover the pieces ($\sim$50 μL). The slow addition of water precipitated the adhesive mixture selectively onto the hydrophobic surfaces, overflowed the cuvette, and caused the pieces to aggregate. We continued to add water ($\sim$50 mL total) in order rinse away all of the excess ethanol and adhesive. The cuvette then contained the liquid-coated pieces and 3 mL of water, to which we added $\sim$50 μL of concentrated NH$_4$OH to promote ionization of the glass surface and discourage the pieces from adhering to the walls of the cuvette.

The cuvette was then attached to a rotor, with the long axis of the cuvette at a $\sim$10° angle relative to the horizon, and rotated at 100–200 rpm for 12–24 h. This rotation enabled the initially formed aggregates to contact one other and coalesce into ordered arrays. After the self-assembly reached completion, the suspension of pieces was deoxygenated by sparging with N$_2$ and exposed to UV radiation ($\lambda \sim$ 254 nm) for $\sim$1 h to polymerize the adhesive. Using a pasteur pipet, we removed a droplet of water containing $\sim$10% of the reaction mixture and placed it onto carbon tape. After drying in air, we examined the sample by optical microscopy and estimated the yield of the experiment by counting $\sim$100 templates and dividing the number of fully formed assemblies by the total number of templates observed. The samples were then sputtered with a thin film of Au and examined using a scanning electron microscope.

(51) Kern, W.; Deckert, C. A. In *Thin Film Processes*; Vossen, J. L., Kern, W., Eds.; Academic Press: San Diego, 1978; pp 401–496.
(52) Evans, S. D.; Sharma, R.; Ulman, A. *Langmuir* **1991**, *7*, 156–161.
(53) Ron, H.; Rubinstein, I. *Langmuir* **1994**, *10*, 4566–4573.
(54) Ron, H.; Matlis, S.; Rubinstein, I. *Langmuir* **1998**, *14*, 1116–1121.
(55) Yan, C.; Golzhauser, A.; Grunze, M.; Woll, C. *Langmuir* **1999**, *15*, 2414–2419.
(56) Woodward, J. T.; Walker, M. L.; Meuse, C. W.; Vanderah, D. J.; Poirier, G. E.; Plant, A. L. *Langmuir* **2000**, *16*, 5347–5353.
(57) Dobbs, D. A.; Bergman, R. G.; Theopold, K. H. *Chem. Eng. News* **1990**, *68*, 2.
(58) Erickson, C. V. *Chem. Eng. News* **1990**, *68*, 2.